Enocyanin promotes osteogenesis and bone regeneration by inhibiting MMP9

WEI MAO[1*], YINFENG ZHENG[1*], WENCONG ZHANG[1*], JINRONG YIN[1], ZHIYI LIU[1], PEILIANG HE[1], GUODONG HOU[1], GUOWEI HUANG[1], HUAN CHEN[1], JUNYAN LIN[1], JIAKE XU[2,3], AIGUO LI[1] and SHENGNAN QIN[1,2,4]

[1]Guangzhou Institute of Traumatic Surgery, Department of Orthopaedics, Guangzhou Red Cross Hospital, Medical College, Jinan University, Guangzhou, Guangdong 510220, P.R. China; [2]School of Biomedical Science, The University of Western Australia, Perth 6009, Australia; [3]Shenzhen Institute of Advanced Technology, Chinese Academy of Sciences, Shenzhen, Guangdong 518055, P.R. China; [4]Monoclonal Antibody Facility, Harry Perkins Institute of Medical Research, Perth 6009, Australia

Received May 23, 2024; Accepted August 29, 2024

DOI: 10.3892/ijmm.2024.5450

Abstract. Enocyanin (ENO), an anthocyanin extracted from grapes, has been shown to exert inhibitory effects on acid phosphatase and inflammation; however, its role in osteogenesis and bone formation is currently unknown. The present study aimed to investigate the effects of ENO on osteogenesis *in vitro* and bone formation *in vivo*, and to explore the rudimentary mechanisms. KusaO cells were employed to evaluate the osteogenic role of ENO *in vitro* by Alizarin red S staining, ALP staining, quantitative PCR and western blotting, and an *in vivo* analysis of the therapeutic effects of ENO on a femoral fracture model was performed using stereo microscope, micro-CT and histological staining. To further investigate the underlying mechanisms, mRNA sequencing was employed to investigate the changes in gene expression and the downstream pathways after ENO treatment. The results showed that ENO could promote the osteogenic differentiation of KusaO cells *in vitro* and bone fracture regeneration *in vivo*. Mechanistically, ENO was highly related to bone formation, including the 'Wnt signalling pathway', 'bone development' and 'bone mineralization'. In addition, matrix metalloproteinase 9 (MMP9) was identified as one of the targets of ENO in its promotional role in osteogenesis. In conclusion, ENO may represent a therapeutic candidate for bone regeneration in bone fractures by regulating osteogenesis and bone formation via MMP9.

Correspondence to: Dr Shengnan Qin, School of Biomedical Science, The University of Western Australia, 6 Verdun Street, Perth 6009, Australia
E-mail: iris.qin@research.uwa.edu.au

Professor Aiguo Li, Guangzhou Institute of Traumatic Surgery, Department of Orthopaedics, Guangzhou Red Cross Hospital, Medical College, Jinan University, 396 Tongfu Middle Road, Guangzhou, Guangdong 510220, P.R. China
E-mail: liaiguo7161@ext.jnu.edu.cn

*Contributed equally

Key words: enocyanin, femur fracture, bone regeneration, osteogenesis, matrix metalloproteinase 9

Introduction

Bones are specialised tissues in the human body, serving not only to protect internal organs, but also to provide essential mechanical support, store minerals and produce blood cells through the process of haematopoiesis (1). Fractures are the most frequent type of traumatic injury and tissue damage, and bones can be restored to their pre-injury state via a process of regeneration. However, ~10% of fractures lead to delayed healing or non-union (2). The process of fracture healing includes several distinct phases, such as inflammation, angiogenesis, cartilage formation, resorption and bone remodelling, as well as several cells, including macrophages, stem cells, osteoblasts and osteoclasts (3,4). Multiple approaches, such as specific biophysical, local and systemic therapies, aim to promote skeletal repair, and the most widely applied strategy is to promote new bone formation (3). For example, the two most extensively studied therapies for promoting fracture healing use bone morphogenetic proteins (BMPs), such as BMP2, and parathyroid hormones (PTHs), such as PTH (1-34), both of which promote new bone formation; however, these strategies still have some limitations (3). Even though both fracture healing and endochondral bone formation have been proven to be directly mediated by BMPs, such as BMP2 (5), it has been reported that BMPs have a lack of effect on shortening the time to fracture union and also on returning bones to their normal function (6).

Therefore, it is important to identify new drugs that can enhance fracture healing with greater effectiveness, improved safety and fewer side effects. Recently, there has been growing interest in naturally occurring compounds that are abundant in food and plants; in particular, anthocyanins (ACNs) have

been reported to serve a role in bone health, which has led to increased attention towards the potential application of these compounds (7). ACNs are water-soluble natural pigments that are prominent in coloured plants and belong to the family of flavonoid compounds (8). Several studies have demonstrated that numerous ACNs can benefit bone homeostasis by promoting the proliferation and differentiation of pre-osteoblasts, and enhancing the maturity of osteoblasts (7). For example, black rice extracts (9) have been shown to promote osteogenesis via Wnt and TGF-β/BMP pathways, and delphinidin-3-rutinoside has been reported to regulate the differentiation and proliferation of osteoblasts through the PI3K/AKT pathway (7,10).

Enocyanin (ENO) is a type of ACN extracted from grape skins, and it exerts inhibitory effects on leucine aminopeptidase, acid phosphatase, γ-glutamyl transpeptidase and esterase activity (11). In addition, it has been shown to possess dose-dependent anti-inflammatory activity in a R3/1-NF-κB luciferase cell model (12). Polyphenols are a class of ubiquitous compounds distributed in nature, with inherent biocompatible, bio-adhesive, antioxidant and antibacterial properties. However, the role of ENO in bone regeneration and fracture healing have yet to be determined.

The present study aimed to investigate the potential role of ENO in promoting osteogenic differentiation *in vitro* and bone regeneration *in vivo*, thereby exploring ENO as a potential candidate for bone fracture management. Furthermore, the underlying mechanism of ENO in osteogenesis was investigated based on mRNA-sequencing analysis.

Materials and methods

Osteogenic induction. The multi-potential bone marrow stromal cell line KusaO was obtained from Dr Julian W Quinn (The University of Melbourne, Melbourne, Australia) and was used for the evaluation of osteogenesis *in vitro* (13). Osteogenic induction was performed as previously described (14). Specifically, cells were cultured at 37˚C and 5% CO_2 in osteogenic medium, which consisted of low glucose (LG)-DMEM (Gibco; Thermo Fisher Scientific, Inc.) supplemented with 10% foetal bovine serum (FBS; Gibco; Thermo Fisher Scientific, Inc.), 100 nM dexamethasone (MilliporeSigma), 50 μM ascorbic acid (MilliporeSigma) and 20 mM β-glycerophosphate (MilliporeSigma). Cells were also cultured in complete medium, which comprised LG-DMEM containing 10% FBS, as a control.

ENO treatment. ENO (CAS no. 11029-12-2; MedChemExpress) at different concentrations (7.5, 15, 30 and 60 μM) was added to the osteogenic medium to evaluate the effect of ENO on the osteogenic differentiation of KusaO cells *in vitro*. The cells were treated for 24, 48 or 72 h to assess cell proliferation, 3 days for reverse transcription-quantitative PCR (RT-qPCR) and alkaline phosphatase (ALP) staining, 7 days for western blotting, and 14 days for alizarin red S (ARS) staining. The medium was replaced every 3 days during the treatment period. The changes in osteoblastic genes were detected using RT-qPCR, and ALP staining was used to assess the osteogenic differentiation of KusaO cells. Western blotting was used to evaluate the protein expression of osteoblastic markers. ARS staining was used to assess the mineralization of KusaO cells.

Cell proliferation. Cell proliferation was assessed using the CellTiter 96® AQueous One Solution Cell Proliferation Assay (MTS) (Promega Corporation) according to the manufacturer's protocol. The cells were seeded at a density of $5x10^3$ cells/well in 96-well plates. After a 24-h incubation, the cells were treated with ENO at various concentrations (7.5, 15, 30 and 60 μM) for 24, 48 and 72 h at 37˚C and 5% CO_2. Subsequently, 10 μl MTS was added to each well and incubated at 37˚C with 5% CO_2 for 4 h. The absorbance was measured at 490 nm using a Bio-Rad 680 microplate reader (Bio-Rad Laboratories, Inc.) and cell proliferation was expressed as a percentage of the control culture value, which was considered 100% viable.

ALP assay. Cells were cultured in osteogenic medium with or without various concentrations of ENO (7.5, 15, 30 and 60 μM) and incubated for 3 days at 37˚C and 5% CO_2. Subsequently, the Alkaline Phosphatase Detection Kit (MilliporeSigma) was used, according to the manufacturer's protocol. Briefly, cells were fixed in 95% ethanol for 10 min at room temperature and were subsequently incubated with ALP regent at 37˚C for another 10 min. After rinsing with PBS; ight microscopy (Nikon Corporation) was used to capture images of the cells with purple ALP staining. To semi-quantify positive ALP staining, Fiji ImageJ2 software was used (15).

ARS staining. Cells were cultured in osteogenic medium containing different concentrations of ENO (0, 7.5, 15, 30 and 60 μM) for 14 days at 37˚C and 5% CO_2. After fixing the cells with 95% ethanol for 10 min at room temperature, they were stained with 0.5% ARS (cat. no. A5533; MilliporeSigma) solution (pH 4.2) for 10 min at room temperature to visualize mineral deposits, which appeared as red-stained areas. Images were captured using a UMAX Scanner (PowerLook 2100XL-USB; VueScan) and a light microscope (Nikon Corporation).

Recombinant MMP9 protein treatment. Cells were cultured in osteogenic medium containing 30 μM ENO, and MMP9 protein (cat. no. 909-MM-010; R&D Systems, Inc.) was added at different concentrations (100 and 200 ng/ml) to observe whether the effects of ENO on osteogenesis could be reversed by MMP9. The cells were treated for 3, 7 or 14 days at 37˚C and 5% CO_2, and the cells were then collected for further RT-qPCR after 3 days, western blotting after 7 days and ARS staining after 14 days to examine changes in osteoblastic genes and proteins, as well as the mineralization of cells.

RT-qPCR. Cells were plated in 24-well plates and were cultured in osteogenic medium containing different concentrations of ENO (0, 15, 30 and 60 μM) for 3 days at 37˚C and 5% CO_2, with 6 replicates for each concentration (n=6). RT-qPCR was performed to detect the changes in the expression levels of osteoblastic genes after ENO treatment, and the experiment was performed as described in our previous study (14). Briefly, total RNA was extracted using TRIzol® (Invitrogen; Thermo Fisher Scientific, Inc.), and cDNA was synthesized with PrimeScript RT Master Mix (cat. no. RR036B; Takara Biotechnology, Ltd.), according to the manufacturers' protocols. The cDNA then underwent qPCR with Power UP SYBR Green Master Mix (cat. no. A25742, Thermo Fisher Scientific,

Table I. Primer sequences.

Primer	Sequence
Gapdh	Forward 5'-AGGTCGGTGTGAACGGATTTG-3'
	Reverse 5'-TGTAGACCATGTAGTTGAGGTCA-3'
Bglap	Forward 5'-TGCTTGTGACGAGCTATCAG-3'
	Reverse 5'-GAGGACAGGGAGGATCAAGT-3'
Alpl	Forward 5'-CCAACTCTTTTGTGCCAGAGA-3'
	Reverse 5'-GGCTACATTGGTGTTGAGCTTTT-3'
Spp1	Forward 5'-AGCAAGAAACTCTTCCAAGCAA-3'
	Reverse 5'-GTGAGATTCGTCAGATTCATCCG-3'
Bsp	Forward 5'-ATGGAGACGGCGATAGTTCC-3'
	Reverse 5'-CTAGCTGTTACACCCGAGAGT-3'
Runx2	Forward 5'-ATGGGACTGTGGTTACCGTCAT-3'
	Reverse 5'-AAGGTGAAACTCTTGCCTCGT-3'
Sp7	Forward 5'-AGCGACCACTTGAGCAAACAT-3'
	Reverse 5'-GCGGCTGATTGGCTTCTTCT-3'

Inc.) on an Analytik Jena qTOWER (Analytik Jena GmbH). The amplification conditions for qPCR were as follow: 50˚C for 2 min and 95˚C for 5 min, followed by 40 cycles at 95˚C for 15 sec and 60˚C for 1 min, with a melt curve stage of 95˚C for 15 sec, 60˚C for 1 min and 95˚C for 15 sec. The relative mRNA expression levels of all genes were normalized to the housekeeping gene Gapdh and were calculated using the $2^{-\Delta\Delta Cq}$ method (16). The primers used were listed in Table I and Mmp9 primers were purchased from Sino Biological, Inc. (cat. no. MP200552).

Western blotting. For western blotting, proteins were extracted from cells with or without treatment using RIPA lysis and extraction buffer (Thermo Fisher Scientific, Inc.) with Halt Protease Inhibitor Cocktail (100X; Thermo Fisher Scientific, Inc.). The concentration of extracted proteins was determined using the BCA Protein Assay (Thermo Fisher Scientific, Inc.), and 20 μg proteins were separated by SDS-PAGE on 10% gels made using TGX FastCast acrylamide kits (Bio-Rad Laboratories, Inc.). The proteins were run alongside a molecular weight marker (Pierce; Thermo Fisher Scientific, Inc.) for 1.5 h at 100 V. The proteins were then transferred from the gel to PVDF membranes using the Trans-Blot Turbo Transfer System (Bio-Rad Laboratories, Inc.). The membranes were incubated in 5% non-fat milk in TBS-1% Tween for 1 h at room temperature and then incubated overnight at 4˚C with primary antibodies against Runx2 (1:1,000; cat. no. 12556; Cell Signaling Technology, Inc.), osteopontin (OPN; 1:1,000; cat. no. ab63856; Abcam) MMP9 (1:500; cat. no. 10375-2-AP; Wuhan Sanying Biotechnology) and β-actin (1:10,000; cat. no. ab32572; Abcam). The next day, the membranes were incubated with HRP-conjugated anti-rabbit and anti-mouse secondary antibodies (1:3,000; cat. nos. 7074 and 7076; Cell Signaling Technology, Inc.) for 1 h at room temperature. For signal development, BeyoECL Plus reagent (Beyotime Institute of Biotechnology) was used according to the manufacturer's recommendations. Images were acquired in the dark using the ChemiDoc XRS Imaging System (Bio-Rad Laboratories, Inc.) and protein expression levels were analysed using Image Lab 5.2.1 software (Bio-Rad Laboratories, Inc.).

RNA-sequencing. Total RNA was extracted from KusaO cells with or without 30 μM ENO treatment under 3-day osteogenic induction using TRIzol. Purity was assessed using a NanoDrop (OD260/280 and OD260/230 ratios; NanoDrop; Thermo Fisher Scientific, Inc.) and integrity was evaluated using an Agilent 4200 TapeStation (Agilent Technologies, Inc.). Libraries were prepared by Chengqi Biotechnology, which involved mRNA isolation, fragmentation and cDNA synthesis. Library quality was assessed using an Agilent 4200 TapeStation. Sequencing was performed on a NovaSeq 6000 platform (Illumina, Inc.) using NovaSeq6000 S4 Reagent kit v1.5 (cat. no. 20028312; Illumina, Inc.), generating 150 bp strand-specific paired-end reads. The loading concentration of the final library was 100 pM.

Bioinformatics analysis. Bioinformatics analysis was carried out by Chengqi Biotechnology. Briefly, raw sequencing reads underwent quality control using FastQC (v0.11.9, https://www.bioinformatics.babraham.ac.uk/projects/fastqc/) and trimming with Trimmomatic (v0.36, http://www.usadellab.org/cms/?page=trimmomatic). Clean reads were aligned to HISAT2 (2.2.0, https://daehwankimlab.github.io/hisat2/). FeatureCounts (v2.0.4, https://subread.sourceforge.net/featureCounts.html) was used to count the read numbers mapped to each gene. Differential expression analysis was conducted with edgeR (v3.40.2, https://bioconductor.org/packages/release/bioc/html/edgeR.html), identifying differentially expressed genes (DEGs) based on a |log2 fold change| >2 and adjusted P<0.05. Functional enrichment analysis of DEGs was subsequently performed. ClusterProfiler R (v4.6.2, https://bioconductor.org/packages/release/bioc/html/clusterProfiler.html) was used to test the statistical enrichment of DEGs in Kyoto Encyclopedia of Genes and Genomes (KEGG) pathways. Gene Set Enrichment Analysis (GSEA) can be used to determine whether a predefined set of genes exhibits statistically significant differences between control and ENO groups. The local version of the GSEA tool was used in the present study (http://www.broadinstitute.org/gsea/index.jsp), and KEGG datasets were used for GSEA.

Femur fracture models. All animal experiments were approved by the Institutional Animal Care and Use Committee of Ruiye Bio-tech Guangzhou Co., Ltd. (approval no. RYEth-20210716213), and were carried out in accordance with The Code of Ethics of the World Medical Association (17). The animal experiments were performed at the animal laboratory of Ruiye Bio-tech Guangzhou Co., Ltd. by the authors. Animals were maintained in a standard room at 22±2˚C with 40-60% humidity, under a 12-h light/dark cycle, with *ad libitum* access to food and water according to the institutional animal guidelines. A total of 12 female Sprague-Dawley rats (weight, 200-250 g) underwent open femoral fracture surgery as previously reported (18). Rats were anesthetized with an intraperitoneal injection of 0.6% pentobarbital sodium (40 mg/kg). Subsequently, the femurs were exposed and cut down the middle to construct femur fracture models. The fractures were then internally fixed using intramedullary

1.2-mm Kirschner wires. After surgery, the rats were housed in individual cages with soft bedding, and easy access to food and water. To minimize the pain of surgery, buprenorphine (0.05 mg/kg) was administered subcutaneously every 8-12 h for 48-72 h post-surgery (17). (The rats were randomly divided into three groups (n=4/group): Saline group, 30 mg/kg ENO group and 60 mg/kg ENO group. After 3 days of recovery from the operation, ENO was injected locally at the fracture sites every 3 days for 6 weeks, with different concentrations used for each group. The Saline group of rats received saline injections as a control.

Stereomicroscopy and micro-CT analysis. A total of 6 weeks after the operation, all rats were sacrificed by an overdose of pentobarbital sodium (0.6%) anaesthesia at a dose of 300 mg/kg by intraperitoneal injection. Death was confirmed by the cessation of heartbeat and respiratory movements, along with the absence of reflexes. Fractured femurs were collected for stereomicroscopy (SMZ25; Nikon Corporation) and were fixed for micro-CT analysis. Femurs were fixed in 10% neutral-buffered formalin solution for 3 days at room temperature. To assess the conditions of bone regeneration, the femurs were scanned using the Skyscan 1176 μCT scanner (Bruker Corporation). Reconstructive images were generated using NRecon v1.6 software (Bruker Corporation) and were then analysed by CTAn v1.9 (Bruker Corporation). Two-and three-dimensional images were generated by Data-viewer and CTvox software (Bruker Corporation), respectively. For bone fracture healing analysis, the defect size of the cortical bone was selected. The bone mass of each group was analysed using CTAn v1.9. The parameters measured included bone volume/tissue volume (BV/TV) and bone mass density (BMD).

Histological staining. After micro-CT scanning, all femurs from the rats were decalcified in 10% EDTA at 37˚C for 10 days followed by 1 month in 10% EDTA. Subsequently, the femurs were processed for paraffin embedding as previously described (19). For further staining, 5-μm sections were utilized. Haematoxylin and eosin (H&E) and Safranin O/Fast green were applied to evaluate the healing of femur fractures as described previously (19), which included bone regeneration and the expression of proteoglycan at the callus bone areas. Images were captured using a stereomicroscope (SMZ25; Nikon Corporation) and a light microscope (Nikon Corporation).

Immunohistochemistry was applied using a Mouse and Rabbit specific HRP/DAB detection IHC kit (cat. no. SAP-9100; OriGene Technologies, Inc.) as described previously (19). Sections were treated according to the manufacturer's protocol, including incubation with primary antibodies overnight at 4˚C. The primary antibodies included OPN (1:200; cat. no. ab63856; Abcam), Collagen I (1:200; cat. no. ab6308; Abcam), Collagen II (1:200; cat. no. 32160702; MilliporeSigma), osteocalcin (OCN; 1:200; cat. no. ab133612; Abcam) and MMP9 (1:200; cat. no. 10375-2-AP; Wuhan Sanying Biotechnology). Images were captured under a light microscope (Nikon Corporation) and were analysed using Fiji ImageJ2 software.

Statistical analysis. Data are presented as the mean ± SD. All data analyses were performed using GraphPad Prism 10.0 (Dotmatics) by one-way ANOVA followed by Dunnett's multiple comparisons test. At least three independent experiments were performed. $P \leq 0.05$ was considered to indicate a statistically significant difference.

Results

ENO enhances proliferation and osteogenesis of KusaO cells in vitro. To investigate the potential impact of ENO on osteoblast differentiation of mesenchymal stem cells (MSCs), KusaO cells, which have multi-differentiation abilities *in vitro* were employed and cultured in either complete medium or osteogenic medium supplemented with different concentrations of ENO (0, 7.5, 15, 30 and 60 μM). To determine whether ENO affected the proliferation of KusaO cells, an MTS assay was used, and the results showed that ENO had no significant effect after 24, 48 or 72 h of treatment (Fig. 1A). ALP is recognized as an important early marker of osteoblast differentiation and was measured to assess the effects of ENO on early osteogenesis. The results showed the levels of ALP were significantly increased in a dose-dependent manner after KusaO cells were treated with different concentrations of ENO (Fig. 1B and C). Additionally, the mineralization of KusaO cells was observed through ARS staining, and the results indicated that ENO significantly increased the mineral deposits of KusaO cells in a dose-dependent manner (Fig. 1D and E). Consistently, RT-qPCR results demonstrated that osteoblastic genes, including Runx2, Alpl, Spp1, Bglap, Bsp and Sp7, were markedly upregulated by 30 μM ENO (Fig. 1F). Western blotting further confirmed that only 30 μM ENO promoted the expression levels of the osteoblastic proteins, Runx2 and OPN, which was consistent with the gene expression findings (Fig. 1G and H). In summary, ENO promoted the osteogenic differentiation of KusaO cells *in vitro*, with the best effects observed in response to 30 μM ENO.

ENO promotes bone regeneration in a rat model of femur fracture. Based on the *in vitro* effects of ENO on promoting the osteoblastic differentiation of KusaO cells, the present study further explored its effects on bone regeneration in a rat model of fracture healing *in vivo*. After 7 days of post-surgery recovery, 30 and 60 mg/kg ENO were injected into the fracture sites. Subsequently, stereomicroscopy, micro-CT and histological staining were applied to detect new bone formation after ENO treatment (Fig. 2A). The stereomicroscope detected bone callus formation at the fracture sites, with little callus formation observed in both ENO groups, whereas more callus formation was found in the Saline group (Fig. 2B). Similarly, the micro-CT showed that the size of bone calluses in the ENO treatment groups was much less than that in the Saline group (Fig. 2D). In addition, non-union was detected in the Saline group, whereas integration at the fracture site was markedly better after ENO treatment (Fig. 2C). Furthermore, bone parameters, including BMD and BV/TV, were significantly increased following ENO treatment, with the best results observed in the 30 mg/kg ENO group (Fig. 2D), suggesting that ENO induced more new bone formation compared with the Saline group. Consistently, H&E staining showed more

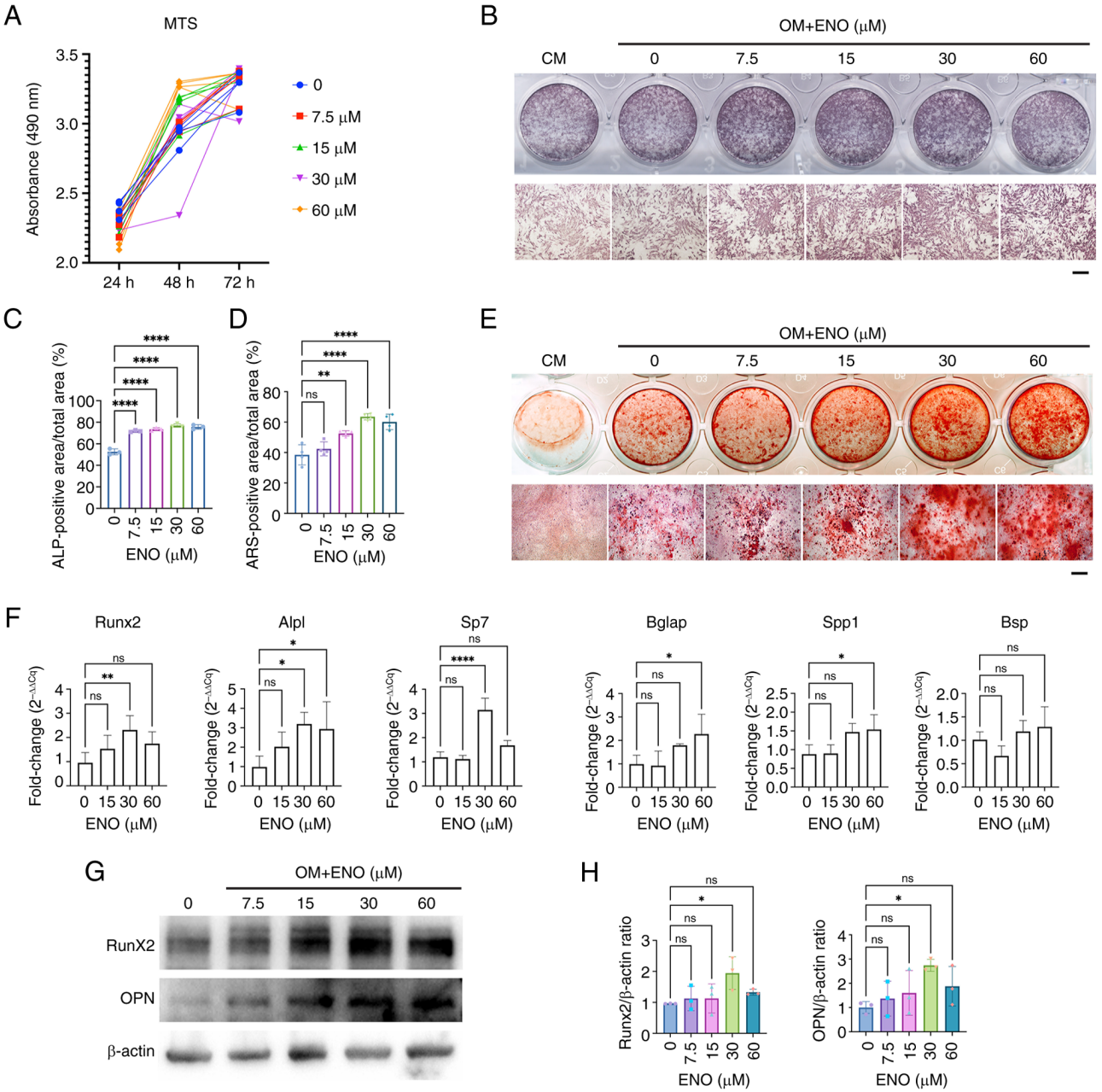

Figure 1. ENO promotes the osteogenesis of KusaO cells *in vitro*. (A) MTS assay of the proliferation of KusaO cells cultured in CM supplemented with different doses of ENO after 24, 48 or 72 h (n=6). (B) ALP staining of KusaO cells after treatment with ENO in CM or OM (n=3). Scale bar, 200 μm. (C) Positive percentage of ALP staining of KusaO cells in each well was semi-quantified by Fiji ImageJ2 (n=3). (D) Percentage of calcium nodules in KusaO cells was semi-quantified after ARS staining (n=4). (E) ARS staining of KusaO cell mineralization after 14 days of osteogenic induction (n=4). Scale bar, 200 μm. Scale bar, 200 μm. (F) Reverse transcription-quantitative PCR analysis of the mRNA expression levels of osteoblastic genes, Alpl, Spp1, Bglap, Runx2, Sp7 and Bsp, in KusaO cells cultured in OM supplemented with different doses of ENO (n=4). The expression levels of genes were normalized to Gapdh and were calculated by $2^{-\Delta\Delta Cq}$. (G) Western blot analysis of the expression of osteoblastic proteins, Runx2 and OPN (n=3). (H) Runx2 and OPN expression levels normalized to β-actin were assessed using Image Lab software (n=3). Data are presented as the mean ± SD. *P<0.05, **P<0.01, ****P<0.0001. ALP, alkaline phosphatase; ARS, Alizarin red S; CM, complete medium; ENO, enocyanin; ns, not significant; OM, osteogenic medium; OPN, osteopontin.

bone formation in the ENO groups compared with that in the Saline group, and woven bone formation was detected in the ENO groups, indicating faster and earlier bone remodelling after ENO treatment (Fig. 2E). Fracture healing is considered the process of endochondral formation, which was measured by Safranin O/Fast Green staining (Fig. 2F); The present results indicated a notable amount of proteoglycan (red), and oval or round chondrocyte-like cells at the bone callus sites in the Saline group, whereas little could be seen in the ENO groups, suggesting that the process of endochondral formation was accelerated by ENO. Notably, 30 mg/kg ENO exhibited the best effects on promoting cartilage resorption and new bone formation.

ENO promotes the expression of osteoblastic proteins at the callus sites of the femur in vivo. Immunohistochemical staining was used to evaluate the expression of osteoblast-related proteins at the callus sites of the femur (Fig. 3). The results

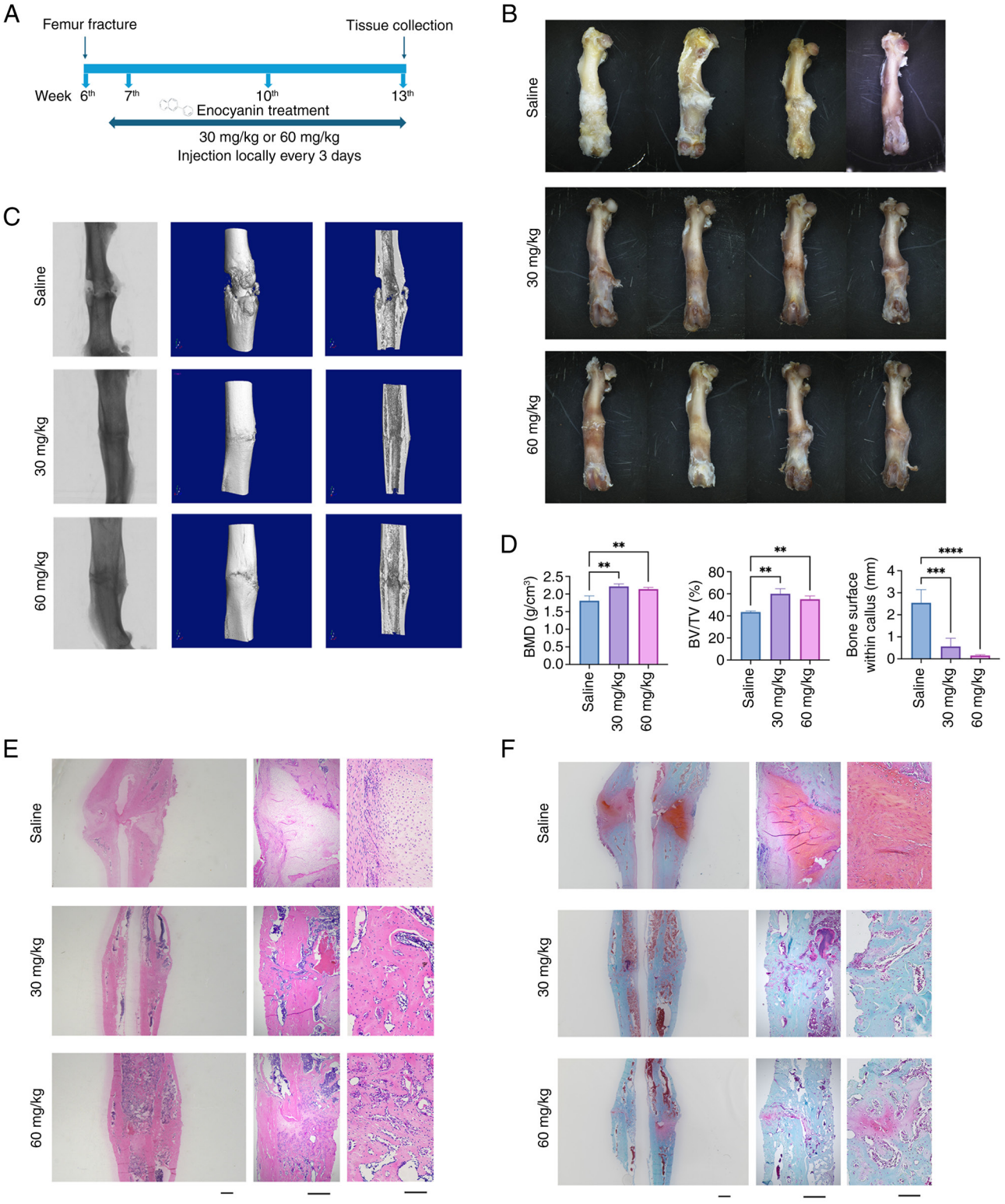

Figure 2. ENO promotes bone regeneration in a rat model of fracture healing. (A) Experimental protocol of establishment of a rat model of femur fracture and the timeline of ENO treatment. (B) Stereomicroscope images of the bone callus outline at the fracture sites (n=4). (C) Representative micro-CT images of the femurs. (D) Quantitative micro-CT analysis of BV/TV, BMD and bone surface of callus sites (n=4). Representative (E) haematoxylin & eosin staining images and (F) Safranin O/Fast Green staining images (n=4). Scale bars, 2,000 μm (left), 500 μm (middle) and 100 μm (right). Data are presented as the mean ± SD. **P<0.01, ***P<0.001, ****P<0.0001. BMD, bone mass density; BV/TV, bone volume/tissue volume; ENO, enocyanin.

showed that ENO not only increased the expression of OCN (Fig. 3A and E), which is a marker of late osteoblastic differentiation, and OPN (Fig. 3B and F), but also decreased collagen II expression (Fig. 3D and H) at the fracture sites. In addition, 60 mg/kg ENO significantly promoted collagen I expression (Fig. 3C and G). Chondrocytes could be seen in the Collagen II-positive areas in the Saline group (black arrows) (Fig. 3D). These findings are consistent with the results of

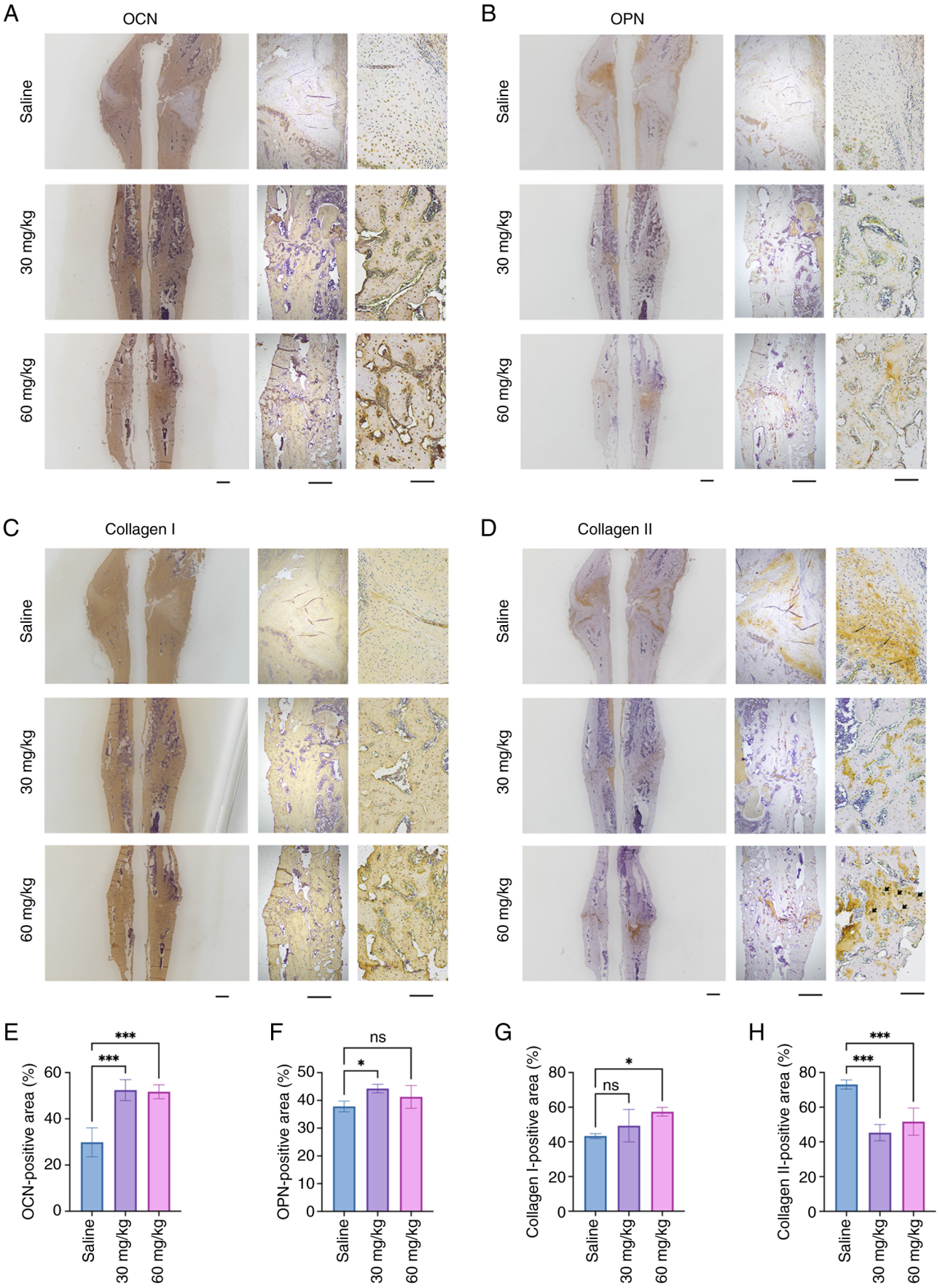

Figure 3. ENO promotes the expression of osteoblastic proteins at the callus sites of the femur *in vivo*. Immunohistochemical analysis was conducted on femur specimens to evaluate the osteogenic effects of ENO. Positive expression of (A) OCN, (B) OPN, (C) Collagen I and (D) Collagen II at the callus sites of the femur with or without ENO treatment (n=4). Scale bars, 2,000 μm (left), 500 μm (middle) and 100 μm (right). Semi-quantification of the positive staining of (E) OCN, (F) OPN, (G) Collagen I and (H) Collagen II using Fiji ImageJ2 software (n=4). Data are presented as the mean ± SD. *P<0.05, ***P<0.001. ENO, enocyanin; ns, not significant; OCN, osteocalcin; OPN, osteopontin.

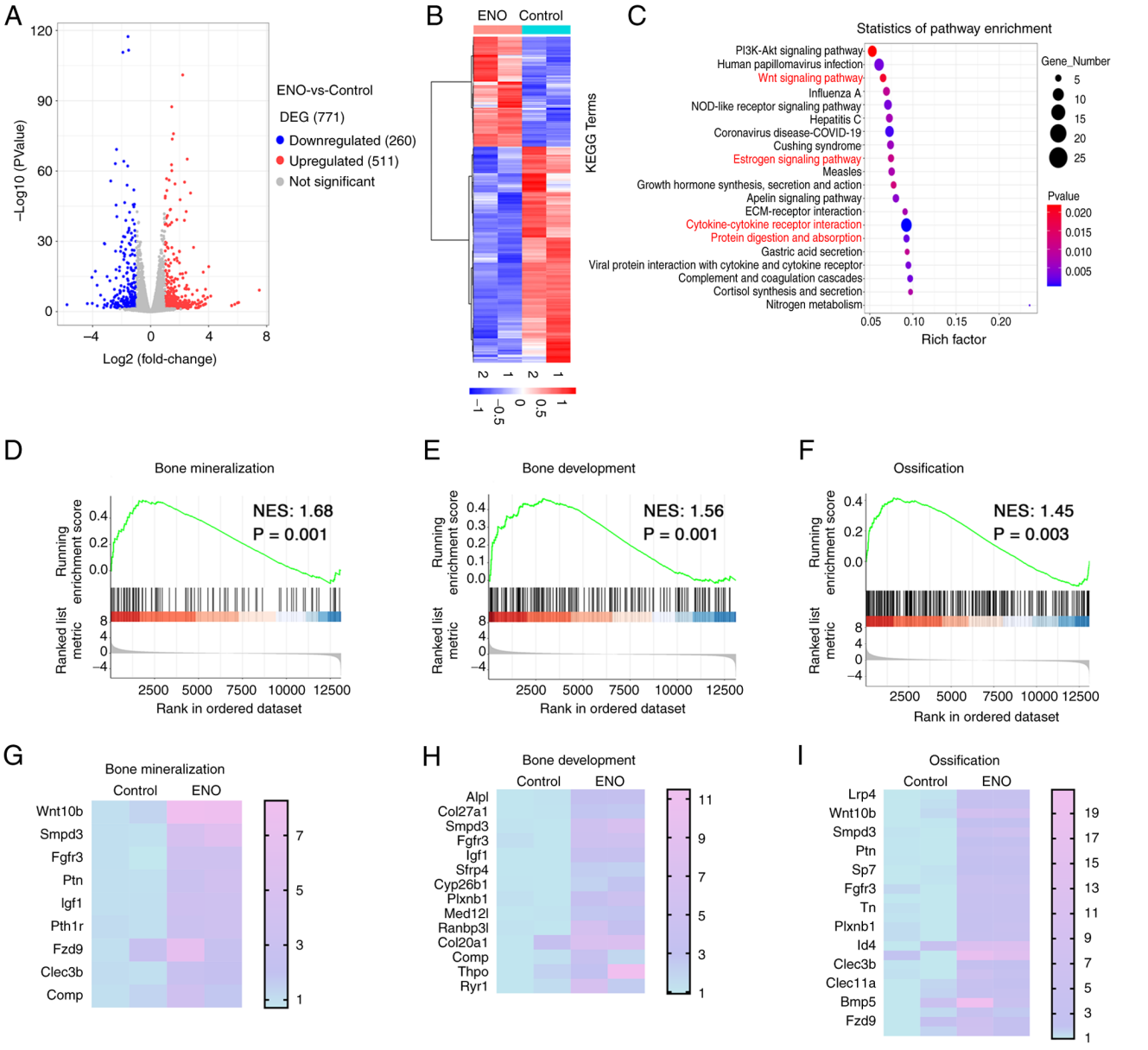

Figure 4. ENO alters the gene expression profiles in KusaO cells induced by osteogenic medium. (A) Volcano plot of the DEGs in KusaO cells following a 3-day treatment with osteogenic medium with or without ENO (n=2). (B) Heatmap of the DEGs between the control and ENO groups (n=2). (C) KEGG pathway enrichment analysis of DEGs. Gene Set Enrichment Analysis showed that (D) 'bone mineralization', (E) 'bone development' and (F) 'ossification' were involved in the role of ENO in osteogenesis. Heatmaps showed the difference in relative gene expression levels associated with (G) 'bone mineralization', (H) 'bone development' and (I) 'ossification' between groups with or without ENO treatment. DEGs were defined by adjusted P<0.05 and |log2 fold change| >2. DEGs, differentially expressed genes; ENO, enocyanin; KEGG, Kyoto Encyclopaedia of Genes and Genomes.

histological staining, which showed reduced cartilage and increased new bone formation after ENO treatment.

ENO alters gene expression profiles in KusaO cells induced by osteogenic medium. To determine the underlying mechanisms governing the effects of ENO on MSC osteogenesis, RNA-sequencing was performed. Total RNA was isolated from cells with or without ENO treatment and RNA-sequencing analysis was then performed. The results showed that 771 DEGs were identified, with 260 genes showing significant downregulation and 511 genes showing upregulation after ENO treatment compared with in the control group (Fig. 4A and B). KEGG analysis revealed that the cells treated with ENO were enriched in the 'Wnt signaling pathway' and 'cytokine-cytokine receptor interaction' pathways, which are classic signalling pathways associated with osteogenesis (20,21) (Fig. 4C). The 'estrogen signalling pathway', which is highly related to osteoporosis, was also involved in the role of ENO. These results highlight the role of ENO in osteogenesis. In addition, 'protein digestion and absorption' was involved in the effect of ENO on KusaO cells induced by osteogenic factors (Fig. 4C), indicating that ENO was involved in regulating matrix degradation. To further identify the gene sets that are related with osteogenesis with or without ENO treatment, GSEA was performed. ENO-induced genes were enriched in 'bone mineralization' (Fig. 4D and E), 'bone development' (Fig. 4F and G) and 'ossification' (Fig. 4H and I), indicating that ENO exerted effects that are highly associated

with osteogenesis and bone formation. Collectively, these RNA-sequencing data showed that ENO may be highly associated with osteogenic differentiation and bone formation.

ENO inhibits MMP9 in osteogenesis in vitro and bone formation in vivo. Since the KEGG pathway analysis showed that 'protein digestion and absorption' was involved in the role of ENO in osteogenesis, proteinase-related genes were selected from the DEGs. Among these genes, Mmp9 was downregulated and Prss35 was upregulated by ENO treatment (Fig. 5A). Mmp9 is known to be associated with endochondral ossification (22), while there is little evidence to support its involvement in osteogenic differentiation. However, there are few reports on Prss35 in bone homeostasis. As such, the present study further examined the mRNA and protein expression levels of MMP9 after ENO treatment *in vitro* and *in vivo*. The results revealed that, *in vitro*, both the mRNA and protein expression levels of MMP9 were decreased after ENO treatment in a dose-dependent manner (Fig. 5B-D). Similarly, *in vivo*, the expression of MMP9 at callus sites was significantly decreased by ENO treatment (Fig. 5E). In the Saline group, MMP9 was strongly expressed at the callus sites, whereas much less MMP9-positive staining could be detected in the ENO groups.

Recombinant MMP9 protein reverses the role of ENO in the osteogenesis of KusaO cells. Based on the findings of RNA-sequencing analysis and confirmation that MMP9 was decreased after ENO treatment, the present study further explored whether MMP9 protein treatment could reverse the role of ENO in the osteogenic differentiation of KusaO cells. The results showed that ENO increased the mineral deposits of KusaO cells, which was consistent with the aforementioned results; however, recombinant MMP9 protein treatment attenuated their mineralization in the presence of ENO (Fig. 6A and 6B). Moreover, the mRNA expression levels of several osteoblastic genes, including Alpl, Runx2, Spp1, Sp7 and Bsp, were downregulated by MMP9 treatment, while there was no significant difference in the mRNA expression levels of Bglap between the groups with or without MMP9 treatment (Fig. 6C). Consistent results were detected regarding the expression levels of osteoblast-related proteins, including Runx2 and OPN, which were significantly decreased by 200 ng/ml MMP9 treatment (Fig. 6D and E).

Discussion

As the global population ages, osteoporosis has emerged as a major health concern, which is a serious condition that can cause bone fractures from even minor trauma, such as coughing. Notably, drugs for osteoporosis, such as denosumab, have been developed to improve bone mineral density and reduce osteoporotic fractures by targeting osteoclasts; however, there are only two therapeutic agents, teriparatide and abaloparatide, that could promote osteoblastic lineage cells (23). Even though efforts have been made in preventing the occurrence of fractures, there were still 178 million new fractures globally in 2019, which represents a 33.4% increase since 1990 (24). Furthermore, osteoporotic fractures are extremely common in worldwide. For example, ~1.5 million individuals suffer from fragility fractures each year in the USA, and one in two women and one in five men aged >50 years will experience an osteoporotic fracture in their lifetime (25). Osteoporosis is also known as a 'silent disease'; patients do not always notice the occurrence of osteoporosis until a fracture happens. Therefore, prevention is considered more important than cure. As such, naturally occurring compounds have attracted increasing attention as a means of preventing and treating osteoporosis, especially fractures.

In the present study, it was revealed that ENO, which belongs to the ACN family, could accelerate osteoblastic differentiation both on the cellular and molecular levels *in vitro*. Furthermore, when rats were treated with ENO, improved fracture healing was observed, with the complete union of fracture sites and increased expression of osteoblast-specific proteins. Based on RNA-sequencing data, it was demonstrated that the roles of ENO in osteogenesis were highly related to Wnt signalling and MMP9 expression levels. Moreover, the present study demonstrated that treatment with the recombinant MMP9 protein could reverse the effects of ENO on osteogenesis. ENO is abundant in foods, such as blackberries and black rice, and its potential role in bone regeneration makes it a promising candidate for fracture healing as a natural remedy (18,26).

ACNs are a class of naturally occurring compounds known for their anti-inflammatory and anti-oxidative effects (27,28). As individuals age, low-grade inflammation and the production of reactive oxygen species increases, leading to an imbalance in bone homeostasis (29). In the present study, it was revealed that ENO promoted the mineralization, as well as the expression levels of osteoblastic genes and proteins *in vitro*, without affecting the proliferation of MSCs. This finding is highly consistent with the effects of other ACNs, such as delphinidin, malvidin and petunidin, which have been reported to positively affect osteoblastic differentiation by upregulating the expression of osteoblastic genes or promoting mineral deposits *in vitro* (30,31). For example, malvidin induced a significantly higher accumulation of calcium deposits in MSCs than untreated MSCs, upregulated osteoblast-specific genes BMP-2 and Runx-2 expression, and induced BMP-2 secretion (30). However, these previous studies were conducted i*n vitro*, and the *in vivo* effect of ACNs on new bone formation remains unexplored.

Based on the effects of ENO on promoting osteogenesis *in vitro*, the present study further explored the roles of ENO in fracture healing *in vivo*. The results showed that ENO significantly accelerated femur fracture healing, as evidenced by improved union of fractures, increased bone mass and expression of osteoblastic proteins. Furthermore, the process of endochondral ossification, new bone formation and cartilage tissue resorption at the callus sites are indicators of bone remodelling during fracture healing, whereas the failure of fracture healing, such as bone non-union, is often due to a lack of initial bone remodelling (32). In the present study, ENO was shown to significantly accelerate the process of bone remodelling, as evidenced by the observation of less proteoglycan and more trabecular bone at the callus sites. Furthermore, the expression of osteoblastic and chondrogenic proteins at the callus sites was highly consistent with the aforementioned findings. Overall, these results suggested that ENO had a

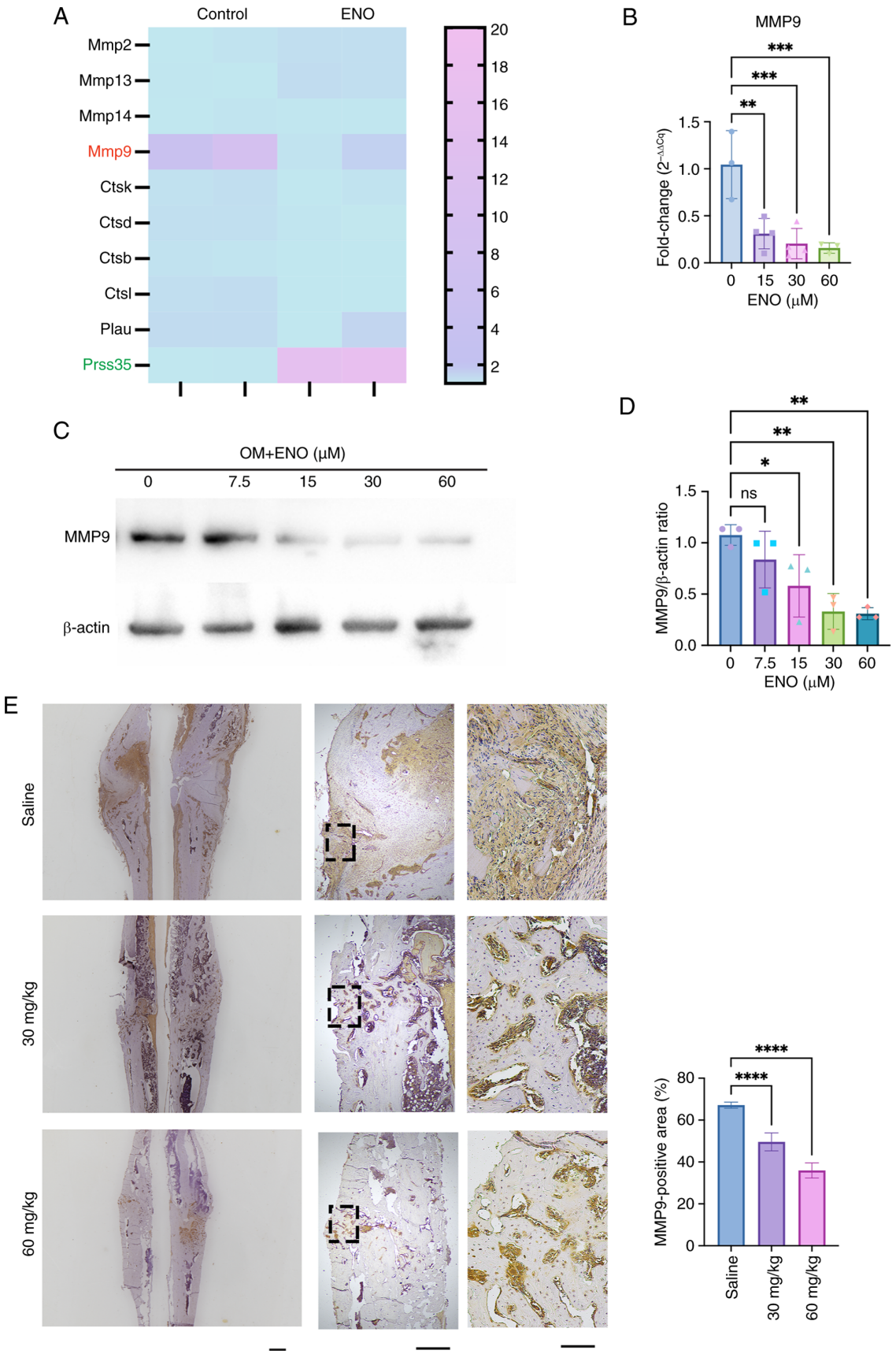

Figure 5. ENO inhibits MMP9 in osteogenesis *in vitro* and bone formation *in vivo*. (A) Heatmap of the differences in the expression of proteinase-related genes in cells with or without ENO treatment in osteogenic medium (n=2). (B) Reverse transcription-quantitative PCR analysis of the mRNA expression levels of Mmp9 after ENO treatment (n=4). (C) Western blot analysis showed that the protein levels of MMP9 decreased after ENO treatment in a dose-dependent manner (n=3). (D) Relative semi-quantification of the expression of MMP9 normalized to β-actin as determined by Image Lab (n=3). (E) Immunohistochemical staining of MMP9 expression at the callus sites in the femur. Scale bars, 2,000 μm (left), 500 μm (middle) and 100 μm (right). Semi-quantification of the positive staining of MMP9 was performed using ImageJ software (n=4). *P<0.05, **P<0.01, ***P<0.001, ****P<0.0001 (n=3). ENO, enocyanin; MMP9, matrix metalloproteinase 9; ns, not significant; OM, osteogenic medium.

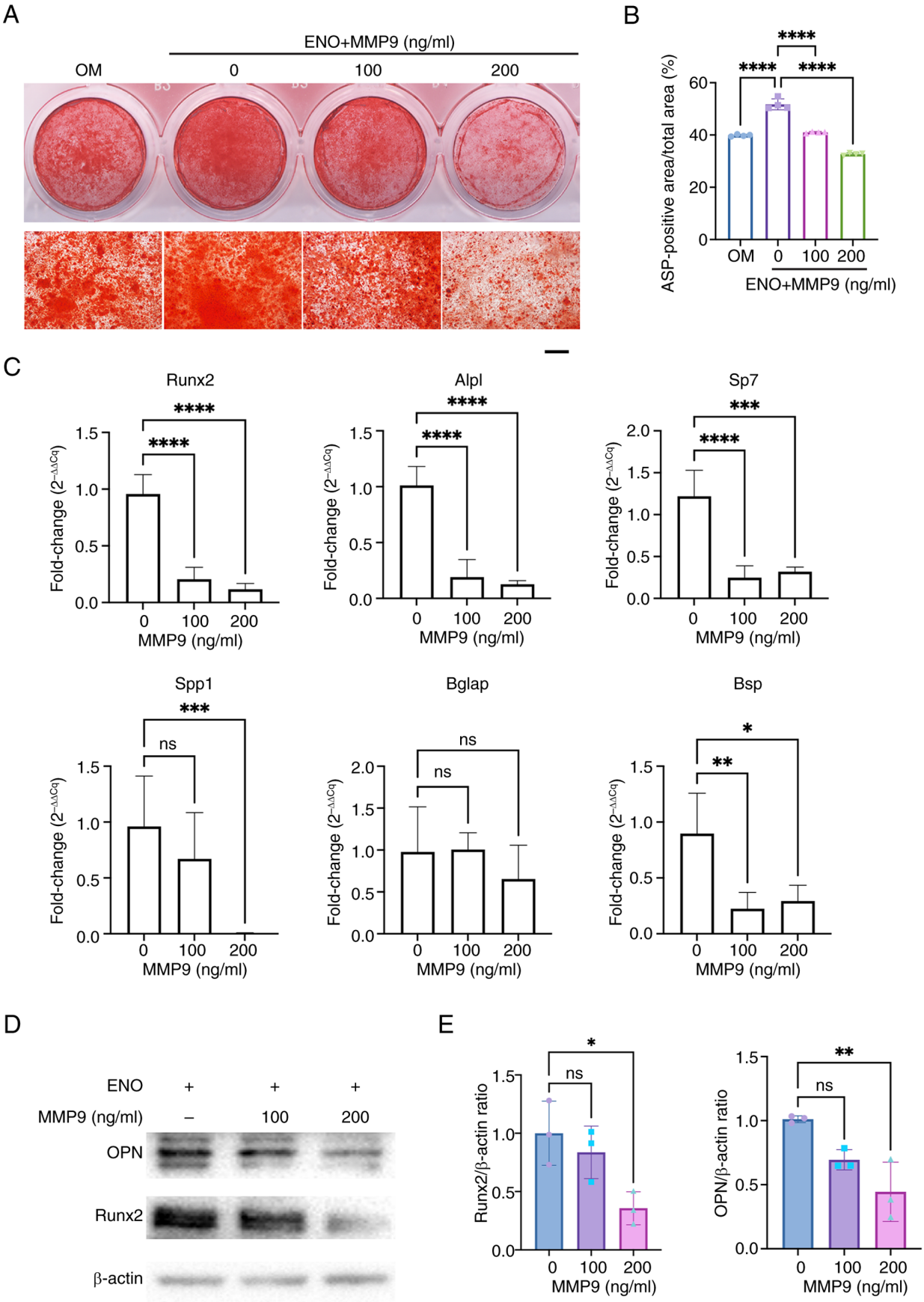

Figure 6. Recombinant MMP9 protein suppresses the osteogenesis of KusaO cells in the presence of ENO. (A) Mineralization after treatment with 30 μM ENO and MMP9 protein (n=4). Scale bar, 500 μm. (B) Percentage of calcium nodules was assessed by Alizarin red S staining and was semi-quantified (n=4). (C) mRNA expression levels of several osteoblastic genes, Alpl, Spp1, Sp7, Runx2, Bglap and Bsp, were downregulated by MMP9 treatment (n=4). (D) Western blot analysis showed that the expression of osteoblast-related proteins, Runx2 and OPN, was dose-dependently decreased by MMP9 treatment (n=3). (E) Relative semi-quantification of the normalized expression of OPN and Runx2 to β-actin was determined by Image Lab (n=3). *P<0.05, **P<0.01, ***P<0.001, ****P<0.0001. ENO, enocyanin; MMP9, matrix metalloproteinase 9; ns, not significant; OPN, osteopontin.

positive impact on fracture healing and could be considered a promising therapeutic agent for the treatment of bone injuries.

To explore the underlying mechanisms of ENO in osteogenesis, RNA-sequencing was performed, which revealed a strong association between ENO, and the 'Wnt signalling pathway' and 'cytokine-cytokine receptor interaction'; both of these are important pathways involved in osteogenic differentiation (20,21). Activating the Wnt or BMP pathway leads to increased bone mass and strength, making it a target for therapeutic intervention in millions of patients at risk of fractures (20,21). GSEA further confirmed that ENO was highly associated with 'bone mineralization', 'bone development' and 'ossification', all of which are known to be involved in osteogenesis and bone formation. These analyses further confirmed that ENO could be a promising candidate for bone regeneration via promoting osteogenesis and new bone formation.

The present study also observed that the KEGG pathway 'protein digestion and absorption' was involved in the osteogenic role of ENO. The *in vivo* data showed that ENO significantly accelerated the bone remodelling process, leading to faster fracture healing. As is well-known, the healing of fractures involves bone formation and bone resorption (32). The proteinases, including MMPs, are a class of enzymes that serve a vital role in various biological processes by cleaving and degrading proteins (33). There are several types of proteinases involved in bone remodelling, including MMPs, serine proteinases, cysteine proteinases and aspartic proteinases, such as cathepsin K (34). Among all of the proteinases known to be involved in bone metabolism and remodelling, there were only two genes, Mmp9 and Prss35, that had significant differences after ENO treatment. The present study further confirmed that ENO inhibited the expression of MMP9 both *in vitro* and *in vivo*. Furthermore, the addition of exogenous MMP9 protein attenuated the ENO-mediated differentiation and mineralization of KusaO cells. These results indicated that MMP9 was involved in the role of ENO in bone remodelling.

MMP9 has a crucial role in regulating the remodelling of skeletal tissues by coordinating matrix degradation, and the recruitment and differentiation of osteoprogenitors (35). However, contrary to expectations, a previous study on Mmp9-knockout mice showed no significant effects on adult bone mass (36). Mmp9 is highly associated with the endochondral ossification process (37,38). Wang *et al* suggested that in $Mmp9^{-/-}$ mice stabilized fractures were healed via endochondral ossification, whereas in wild-type mice they were healed via intramembranous ossification (37). In addition, in another study, Mmp2 was shown to be involved in intramembranous ossification, whereas Mmp9 could specifically impact the endochondral ossification process (38,39). Therefore, ENO may facilitate the process of cartilage formation by decreasing MMP9 expression, which in turn could increase new bone formation.

Notably, Mmp9 is released by osteoclasts, suggesting that it may participate in the intracellular communication between osteoblasts and osteoclasts, which is crucial in bone remodelling (40,41). Nevertheless, a previous study indicated that Mmp9-null osteoclast fusion and function are largely unaffected *in vitro* or *in vivo* (36), suggesting that the role of Mmp9 in bone may not specifically target osteoclasts. Given this, we aimed to knockdown Mmp9 in KusaO cells, in order to further confirm the role of MMP9 in osteogenesis; however, it was found that KusaO cells without osteogenic induction did not express Mmp9 (data not shown).

One limitation of the present study is that the role of ENO was not explored in osteoporotic fractures, even though ENO was revealed to be closely associated with Wnt signalling, protein digestion and absorption pathways, and oestrogenic signalling, which also have fundamental effects on osteoporotic fracture healing. The reason why we did not explore the role of ENO in osteoporotic fractures is because hyperactive osteoclasts serve a crucial role under osteoporotic conditions, and we did not observe significant effects of ENO on osteoclastogenesis (data not shown). However, the effects of ENO on bone resorption of mature osteoclasts have not yet been investigated, and thus further experiments are needed in the future to explore this possibility.

In conclusion, in the present study it was observed that ENO had a positive effect on the osteoblastic differentiation of MSCs *in vitro*, and it also promoted fracture healing of the femur *in vivo*. The mechanisms involved in the role of ENO in osteogenesis included the activation of Wnt signalling, and the regulation of protein digestion and absorption pathways, all of which have vital roles in bone remodelling. Additionally, the present results suggested that Mmp9 might be a target of ENO in promoting bone defect healing.

Acknowledgements

The authors would like to acknowledge the equipment support from Professor Kathleen Davern, Dr Kevin Li and Dr Quang Nguyen (Harry Perkins Institute of Medical Research), and Professor Kathy Fuller (School of Biomedical Science, The University of Western Australia).

Funding

This work was supported by the Guangzhou Science and Technology Project (grant nos. 202002030049 and 2023A03 J0987) and the Oversea Study Program of Guangzhou Elite Project to SQ.

Availability of data and materials

The data generated in the present study may be found in the NCBI public database under accession number PRJNA1138174 or at the following URL: https://www.ncbi.nlm.nih.gov/bioproject/?term=PRJNA1138174. The other data generated in the present study may be requested from the corresponding author.

Authors' contributions

SNQ, JKX and AGL contributed to the study design. WM, YFZ, WCZ, JRY, ZYL, PLH, GDH, GWH, HC and JYL carried out experiments. HC, GDH, WM, PLH, WCZ, ZYL and GWH contributed to data collection and analysis. WM, SNQ and AGL contributed to the drafting and revision of the manuscript. SNQ and AGL confirm the authenticity of all the raw data. All authors read and approved the final version of the manuscript.

Ethics approval and consent to participate

All animal experiments were approved by the Institutional Animal Care and Use Committee of Ruiye Bio-tech Guangzhou Co., Ltd. (approval no. RYEth-20210716213), and were carried out in accordance with The Code of Ethics of the World Medical Association.

Patient consent for publication

Not applicable.

Competing interests

The authors declare that they have no competing interests.

References

1. Maksimkin AV, Senatov FS, Anisimova NY, Kiselevskiy MV, Zalepugin DY, Chernyshova IV, Tilkunova NA and Kaloshkin SD: Multilayer porous UHMWPE scaffolds for bone defects replacement. Mater Sci Eng C Mater Biol Appl 73: 366-372, 2017.
2. Ho-Shui-Ling A, Bolander J, Rustom LE, Johnson AW, Luyten FP and Picart C: Bone regeneration strategies: Engineered scaffolds, bioactive molecules and stem cells current stage and future perspectives. Biomaterials 180: 143-162, 2018.
3. Einhorn TA and Gerstenfeld LC: Fracture healing: Mechanisms and interventions. Nat Rev Rheumatol 11: 45-54, 2015.
4. Murata K, Ito H, Yoshitomi H, Yamamoto K, Fukuda A, Yoshikawa J, Furu M, Ishikawa M, Shibuya H and Matsuda S: Inhibition of miR-92a enhances fracture healing via promoting angiogenesis in a model of stabilized fracture in young mice. J Bone Miner Res 29: 316-326, 2014.
5. Axelrad TW and Einhorn TA: Bone morphogenetic proteins in orthopaedic surgery. Cytokine Growth Factor Rev 20: 481-488, 2009.
6. Aro HT, Govender S, Patel AD, Hernigou P, Perera de Gregorio A, Popescu GI, Golden JD, Christensen J and Valentin A: Recombinant human bone morphogenetic protein-2: a randomized trial in open tibial fractures treated with reamed nail fixation. J Bone Joint Surg Am 93: 801-808, 2011.
7. Mao W, Huang G, Chen H, Xu L, Qin S and Li A: Research progress of the role of anthocyanins on bone regeneration. Front Pharmacol 12: 773660, 2021.
8. Levis S and Lagari VS: The role of diet in osteoporosis prevention and management. Curr Osteoporos Rep 10: 296-302, 2012.
9. Jang WS, Seo CR, Jang HH, Song NJ, Kim JK, Ahn JY, Han J, Seo WD, Lee YM and Park KW: Black rice (Oryza sativa L.) extracts induce osteoblast differentiation and protect against bone loss in ovariectomized rats. Food Funct 6: 265-275, 2015.
10. Casati L, Pagani F, Fibiani M, Lo Scalzo R and Sibilia V: Potential of delphinidin-3-rutinoside extracted from Solanum melongena L. as promoter of osteoblastic MC3T3-E1 function and antagonist of oxidative damage. Eur J Nutr 58: 1019-1032, 2019.
11. Sako F, Kobayashi N, Taniguchi N and Takakuwa E: A study on the toxicity of natural food dyes-toxicity and enzyme inhibition in Paramecium caudatum. J Toxicol Sci 3: 127-136, 1978.
12. Della Vedova L, Ferrario G, Gado F, Altomare A, Carini M, Morazzoni P, Aldini G and Baron G: Liquid Chromatography-High-Resolution Mass Spectrometry (LC-HRMS) profiling of commercial enocianina and evaluation of their antioxidant and anti-inflammatory activity. Antioxidants (Basel) 11: 1187, 2022.
13. Nakamura A, Ly C, Cipetić M, Sims NA, Vieusseux J, Kartsogiannis V, Bouralexis S, Saleh H, Zhou H, Price JT, *et al*: Osteoclast inhibitory lectin (OCIL) inhibits osteoblast differentiation and function in vitro. Bone 40: 305-315, 2007.
14. Qin S, Wang W, Liu Z, Hua X, Fu S, Dong F, Li A, Liu Z, Wang P, Dai L, *et al*: Fibrochondrogenic differentiation potential of tendon-derived stem/progenitor cells from human patellar tendon. J Orthop Translat 22: 101-108, 2020.
15. Schindelin J, Arganda-Carreras I, Frise E, Kaynig V, Longair M, Pietzsch T, Preibisch S, Rueden C, Saalfeld S, Schmid B, *et al*: Fiji: An open-source platform for biological-image analysis. Nat Methods 9: 676-682, 2012.
16. Livak KJ and Schmittgen TD: Analysis of relative gene expression data using real-time quantitative PCR and the 2(-Delta Delta C(T)) Method. Methods 25: 402-408, 2001.
17. Guideline-Rodent Analgesia (Procedure Specific), T.u.o. queensland, Editor. 2022.
18. Xu L, Huang S, Hou Y, Liu Y, Ni M, Meng F, Wang K, Rui Y, Jiang X and Li G: Sox11-modified mesenchymal stem cells (MSCs) accelerate bone fracture healing: Sox11 regulates differentiation and migration of MSCs. FASEB J 29: 1143-1152, 2015.
19. Wang W, Qin S, He P, Mao W, Chen L, Hua X, Zhang J, Xiong X, Liu Z, Wang P, *et al*: Type II collagen sponges facilitate tendon stem/progenitor cells to adopt more chondrogenic phenotypes and promote the regeneration of fibrocartilage-like tissues in a rabbit partial patellectomy model. Front Cell Dev Biol 9: 682719, 2021.
20. Baron R and Kneissel M: WNT signaling in bone homeostasis and disease: From human mutations to treatments. Nat Med 19: 179-192, 2013.
21. Lowery JW and Rosen V: The BMP pathway and its inhibitors in the skeleton. Physiol Rev 98: 2431-2452, 2018.
22. Page-McCaw A, Ewald AJ and Werb Z: Matrix metalloproteinases and the regulation of tissue remodelling. Nat Rev Mol Cell Biol 8: 221-233, 2007.
23. Reid IR and Billington EO: Drug therapy for osteoporosis in older adults. Lancet 399: 1080-1092, 2022.
24. GBD 2019 Fracture Collaborators: Global, regional, and national burden of bone fractures in 204 countries and territories, 1990-2019: A systematic analysis from the Global Burden of Disease Study 2019. Lancet Healthy Longev 2: e580-e592, 2021.
25. Clynes MA, Harvey NC, Curtis EM, Fuggle NR, Dennison EM and Cooper C: The epidemiology of osteoporosis. Br Med Bull 133: 105-117, 2020.
26. He J, Li X, Wang Z, Bennett S, Chen K, Xiao Z, Zhan J, Chen S, Hou Y, Chen J, *et al*: Therapeutic anabolic and anticatabolic benefits of natural Chinese Medicines for the treatment of osteoporosis. Front Pharmacol 10: 1344, 2019.
27. Lee YM, Yoon Y, Yoon H, Park HM, Song S and Yeum KJ: Dietary anthocyanins against obesity and inflammation. Nutrients 9: 1089, 2017.
28. Samarpita S, Ganesan R and Rasool M: Cyanidin prevents the hyperproliferative potential of fibroblast-like synoviocytes and disease progression via targeting IL-17A cytokine signalling in rheumatoid arthritis. Toxicol Appl Pharmacol 391: 114917, 2020.
29. Domazetovic V, Marcucci G, Iantomasi T, Brandi ML and Vincenzini MT: Oxidative stress in bone remodeling: Role of antioxidants. Clin Cases Miner Bone Metab 14: 209-216, 2017.
30. Saulite L, Jekabsons K, Klavins M, Muceniece R and Riekstina U: Effects of malvidin, cyanidin and delphinidin on human adipose mesenchymal stem cell differentiation into adipocytes, chondrocytes and osteocytes. Phytomedicine 53: 86-95, 2019.
31. Azuma K, Ohyama A, Ippoushi K, Ichiyanagi T, Takeuchi A, Saito T and Fukuoka H: Structures and antioxidant activity of anthocyanins in many accessions of eggplant and its related species. J Agric Food Chem 56: 10154-10159, 2008.
32. Marsell R and Einhorn TA: The biology of fracture healing. Injury 42: 551-555, 2011.
33. Paiva KBS and Granjeiro JM: Matrix metalloproteinases in bone resorption, remodeling, and repair. Prog Mol Biol Transl Sci 148: 203-303, 2017.
34. Delaissé JM, Engsig MT, Everts V, del Carmen Ovejero M, Ferreras M, Lund L, Vu TH, Werb Z, Winding B, Lochter A, *et al*: Proteinases in bone resorption: obvious and less obvious roles. Clin Chim Acta 291: 223-234, 2000.
35. Ortega N, Behonick D, Stickens D and Werb Z: How proteases regulate bone morphogenesis. Ann N Y Acad Sci 995: 109-116, 2003.
36. Zhu L, Tang Y, Li XY, Keller ET, Yang J, Cho JS, Feinberg TY and Weiss SJ: Osteoclast-mediated bone resorption is controlled by a compensatory network of secreted and membrane-tethered metalloproteinases. Sci Transl Med 12: eaaw6143, 2020.

37. Wang X, Yu YY, Lieu S, Yang F, Lang J, Lu C, Werb Z, Hu D, Miclau T, Marcucio R and Colnot C: MMP9 regulates the cellular response to inflammation after skeletal injury. Bone 52: 111-119, 2013.
38. Kalev-Altman R, Janssen JN, Ben-Haim N, Levy T, Shitrit-Tovli A, Milgram J, Shahar R, Sela-Donenfeld D and Monsonego-Ornan E: The gelatinases, matrix metalloproteinases 2 and 9, play individual roles in skeleton development. Matrix Biol 113: 100-121, 2022.
39. Vu TH, Shipley JM, Bergers G, Berger JE, Helms JA, Hanahan D, Shapiro SD, Senior RM and Werb Z: MMP-9/gelatinase B is a key regulator of growth plate angiogenesis and apoptosis of hypertrophic chondrocytes. Cell 93: 411-422, 1998.
40. Cao X: Targeting osteoclast-osteoblast communication. Nat Med 17: 1344-1346, 2011.
41. Kular J, Tickner J, Chim SM and Xu J: An overview of the regulation of bone remodelling at the cellular level. Clin Biochem 45: 863-873, 2012.